Published in final edited form as:
J Immunol. 2014 July 15; 193(2): 571–579. doi:10.4049/jimmunol.1400043.

TCR affinity and tolerance mechanisms converge to shape T cell diabetogenic potential

Maria Bettini[*,1], **Lori Blanchfield**[†], **Ashley Castellaw**[*], **Qianxia Zhang**[*,2], **Maki Nakayama**[‡], **Matthew P. Smeltzer**[§], **Hui Zhang**[§], **Kristin A. Hogquist**[¶], **Brian D. Evavold**[†], and **Dario A. A. Vignali**[*,2]

[*]Department of Immunology, St. Jude Children's Research Hospital, Memphis, TN 38105

[†]Department of Microbiology and Immunology, Emory University, Atlanta, GA 30322

[‡]Barbara Davis Center for Childhood Diabetes, University of Colorado Denver, Aurora, CO 80045

[§]Department of Biostatistics, St. Jude Children's Research Hospital, Memphis, TN 38105

[¶]Department of Laboratory Medicine and Pathology, University of Minnesota, Minneapolis, MN 55414, USA

Abstract

Autoreactive T cells infiltrating the target organ can possess a broad TCR affinity range. However, the extent to which such biophysical parameters contribute to T cell pathogenic potential remain unclear. In this study, we selected eight $InsB_{9\text{-}23}$-specific TCRs cloned from $CD4^+$ islet-infiltrating T cells that possessed a relatively broad range of TCR affinity to generate non-obese diabetic (NOD) TCR retrogenic mice. These TCRs exhibited a range of 2D affinities (~10^{-4} - 10^{-3} μm^4) that correlated with functional readouts and responsiveness to activation *in vivo*. Surprisingly, both higher and lower affinity TCRs could mediate potent insulitis and autoimmune diabetes suggesting that TCR affinity does not exclusively dictate or correlate with diabetogenic potential. Both central and peripheral tolerance mechanisms selectively impinge on the diabetogenic potential of high affinity TCRs, mitigating their pathogenicity. Thus, TCR affinity and multiple tolerance mechanism converge to shape and broaden the diabetogenic T cell repertoire, potentially complicating efforts to induce broad, long-term tolerance.

Introduction

T cell receptor (TCR) affinity is a key parameter that dictates T cell fate decisions during development in the thymus and after encounter with antigens in the periphery. As a mechanism to prevent self-reactivity and autoimmunity, negative selection of high affinity TCRs in the thymus results in efficient deletion of high affinity self-reactive T cells (1-5). Therefore, the majority of self-reactive T cells involved in autoimmune disease have escaped thymic selection due to the lower affinity of their TCRs and/or the lack of tissue

Correspondence: vignali.lab@stjude.org.
[1]Department of Pediatrics, Baylor College of Medicine, Houston, TX 77030;
[2]Department of Immunology, University of Pittsburgh School of Medicine, Pittsburgh, PA 15261.

specific antigen expressed in the thymus. These two mechanisms of escape can potentially result in a self-reactive population of T cells with variable TCR affinities. However, it is unclear whether the lower affinity TCRs can equally contribute to organ destruction compared to higher affinity autoreactive TCRs.

Autoimmune processes, in particular type 1 diabetes, are in most cases chronic and slow developing disorders where diagnosis comes years after antigen specific antibodies are first detected in the serum. The chronic nature of the disease and the fact that there is an accumulation of antigenic targets in type 1 diabetes suggests a dynamic T cell response with recruitment of new cells throughout the process. Multiple regulatory mechanisms, such as cell intrinsic negative regulators and cell extrinsic regulatory T cells, can modulate and to some degree control activation of pathogenic T cells. However, it is still unknown why some T cells are (a) more likely to escape central and peripheral tolerance mechanisms, (b) more pathogenic and (c) more efficient mediators of beta cell destruction. It is also unclear whether TCR affinity can be a predictor of T cell pathogenicity in type 1 diabetes.

Several lines of evidence, most of these obtained with MHC class I-restricted TCRs, suggest that higher affinity self-reactive T cells are more pathogenic in autoimmune disease models (6). Studies performed in mice and humans have shown a progressive increase in TCR avidity over the course of diabetes development (7, 8). However, $CD4^+$ T cell responses to infection retain clonotypic diversity and a range of TCR affinities (9), and a recent study has shown that an autoimmune $CD4^+$ T cell response to a single myelin epitope comprises of a wide range of affinities (10). Most studies on autoimmune TCR affinity have utilized either model antigen systems or were limited to few T cell receptors at a time, which gives a limited snapshot of a TCR repertoire present in autoimmunity. The question then remains whether the TCR affinity is a good predictor of $CD4^+$ T cell function and whether higher or the lower affinity $CD4^+$ T cells are the drivers of an autoimmune response.

Surface Plasmon Resonance (SPR) has traditionally been used to define TCR affinity and other biophysical measurements based on a free flowing ligand binding to a receptor immobilized on a sensor surface. In order to enhance physiological relevance, the two-dimensional (2D) micropipette adhesion frequency assay calculates an effective TCR affinity on the cell surface where both receptor and ligand are presented in cell membranes and are brought into proximity in a two-dimensional space (11). Additionally, SPR necessitates the use of purified TCR, which has been the limiting factor in assessing affinity for multiple TCRs. The 2D micropipette adhesion frequency assay eliminates the TCR purification step because T cells are utilized for affinity determination of multiple TCRs specific to the same antigenic peptide epitope with sensitivity to a single TCR:pMHC bond. This technique has been highly predictive of the functional outcome of TCR ligation in $CD4^+$ and $CD8^+$ T cells (12-15).

We focused our analysis on the dominant epitope of insulin, a target antigen in autoimmune diabetes in NOD mice and in type 1 diabetes humans, and obtained a panel of eight $InsB_{9\text{-}23}$-specific MHC II restricted TCRs, most of which were cloned from T cells infiltrating the pancreatic islets. We performed biophysical and biological measurements of relative TCR affinities, and then assessed these TCRs for their *in vivo* function and

pathogenicity in autoimmune diabetes to determine the parameters that shape TCR diabetogenic potential.

Materials and Methods

2D TCR affinity measurements

The details of the micropipette adhesion frequency assay are described in detail elsewhere (13, 16). In brief, a pMHC-coated RBC and T cell were placed on opposing micropipettes and mechanically brought into contact for a controlled contact area (A_c) and time (t). The T cell was retracted at the end of the contact period, and the presence of adhesion (indicating TCR–pMHC ligation) was observed microscopically by elongation of the RBC membrane. This contact– retraction cycle was performed 50 times per T cell–RBC pair to calculate an adhesion frequency (P_a). For each experiment, a mean Pa was calculated based on T cells that bound specifically to antigen. The population-averaged 2D affinity (A_cK_a) using the mean Pa at equilibrium (where $t \rightarrow \infty$) was calculated using the following equation: $A_cK_a = \ln[1-P_a(\infty)]/(m_rm_l)$, where m_r and m_l reflect the receptor (TCR) and ligand (pMHC) densities, respectively. Insulin peptide/MHC monomers used in the micropipette analyses were previously published (17) and provided by NIH tetramer core.

Mice

NOD.*scid* and NOD/ShiLtJ mice were obtained from The Jackson Laboratories. All mice were bred and housed at the St. Jude Animal Resources Center (Memphis, TN) in a Helicobacter-free specific pathogen-free facility following state, national, and institutional mandates. NOD.129S2(B6)-Ins2tm1Jja/GseJ (referred to as NOD.*Ins2*$^{-/-}$ mice), originally obtained from Jackson laboratories, NOD.Foxp3^{DTR} mice originally obtained from JDRF repository (18) and C57BL/6-Tg(Nr4a1-EGFP/cre)820Khog/J (referred to as Nur77^{GFP}) were crossed in our facility to NOD.*scid* mice (99.3% NOD by SNP analysis). All animal experiments were preformed in an AAALAC-accredited, SPF facility following national, state and institutional guidelines. Animal protocols were approved by the St. Jude Institutional Animal Care and Use Committee.

Cloning of P2 TCR from pancreatic islets

CD4$^+$ T cells were isolated from the islets of WT NOD mice (10 weeks of age), expanded *in vitro* with PMA and ionomycin, then sorted based on insulin tetramer binding and fused with a fusion partner expressing an IL-2 GFP reporter facilitating screening of the clones for antigen sensitivity. P2 TCR was cloned from the hybrid clone that screened positive for sensitivity to $InsB_{9\text{-}23}$ peptide stimulation.

TCR reagents and retroviral-mediated stem cell gene transfer

All the TCRs used for this study were chosen based on their ability to mediate T cell expansion or IL-2 secretion in response to wild type $lnsB_{9\text{-}23}$ peptide. Most of the TCRs used in this study were derived from islet-infiltrating T cells (Supplemental Table I). Generation of retroviral TCR retroviral constructs and TCR retrogenic mouse generation has been previously published (19-23). Briefly, female NOD.*scid* mice were injected i.p. with 150 mg/kg of 5-fluorouracil (American Pharmaceutical Partners Inc, Schaumburg, IL); bone

marrow was harvested 72 hours later and cultured for 24 hours in complete DMEM supplemented with 20 % FBS, 20 ng/ml IL-3, 50 ng/ml hIL-6 and 50 ng/ml MSCF (R&D Systems, Minneapolis, MN). Bone marrow cells were spin transduced with retroviral supernatant, 6μg/ml polybrene, and freshly added cytokines for 1 hour at 37°C at 2500rpm at 24 and 48 hours, fresh media was added at 72 hours. After 96 hours, bone marrow cells were injected at about 2×10^6 cells per recipient (~1 donor/1 recipient). Mice were test-bled for TCR reconstitution 8 weeks post-transplant for diabetes analysis, and analyzed 8 weeks post-transplant for all other experiments. The 12-4.4m1 sequence used in this study was an artificially modified version of 12-4.4 (see Supplemental Table I).

Islet isolation

Pancreata were perfused by injecting 3 mL collagenase 4 (Worthington, Lakewood, NJ) (400 units/mL in Hanks' balanced salt solution (HBSS) and 10% fetal bovine serum (FBS)), harvested, and placed in 3–5 mL collagenase 4. The pancreata then were incubated at 37°C for 25 min, after which they were washed three times with 7 mL 5% FBS/HBSS and resuspended in 10 mL 5% FBS/HBSS. Islets were handpicked and incubated at 37°C for 15 min in 1 mL cell dissociation buffer (Invitrogen, Carlsbad, CA) and then further dissociated by vortexing and pipetting. Cells were then washed in 10 mL 5% FBS/HBSS, counted, and analyzed by flow cytometry.

Assessment of insulitis and diabetes

Pancreata of mice were harvested at 8-9 weeks post bone marrow transfer. Paraffin embedded 4-μm-thick step section were cut at 150-μm apart and stained with hematoxylin and eosin at the St. Jude Histology Core Facility. Islets (50–90 per mouse) were scored in a blinded manner using the method outlined in Current Protocols in Immunology (24). Diabetes incidence was monitored weekly by testing for the presence of glucose in the urine by Diastix® (Bayer, Elkhart, IN). Mice testing positive by Diastix® then were tested with a Breeze2® glucometer (Bayer, Elkhart, IN) for elevated blood glucose levels and were considered diabetic if their blood glucose was >400 mg/dL.

T cell line development and in vitro stimulation

TCR^- 4G4.$CD4^+$ T cell hybridoma line was transfected with TCRs and sorted on an identical narrow range of TCR expression. 50,000 TCR transfectants were stimulated with 200,000 NOD splenocytes and $InsB_{9\text{-}23}$. Phospho-Erk expression was analyzed with after 1% formaldehyde fixation and methanol permeabilization. IL-2 secretion was analyzed after 24 hours via IL-2 ELISA.

In order to generate T cells lines, splenocytes from NOD.*scid* or NOD.*scid*.$Nur77^{GFP}$ TCR retrogenic mice were sorted on $CD4^+Ametrine^+$ cells and expanded *in vitro* with 1μg/mL ionomycin, 10ng/mL PMA (Sigma), and 1000units/mL hIL-2 for 2 days. Media was changed every two days and replenished with 1000units/mL hIL-2. After 10-14 day expansion, cells were used for 2D measurements, or in stimulation assays. 25,000 NOD.*scid*.$Nur77^{GFP}$ T cells were stimulated in 96 flat bottom plate with plate bound αCD3, or in 96 u-bottom plate with 200,000 NOD splenocytes as a source of APCs that were pre-incubated with 10μM $InsB_{9\text{-}23}$, 2.5 units/mL Humulin®, 200,000 islet cells from NOD

female mice 16 hours prior to stimulation. After 24 hour stimulation, cells were stained for CD4 and analyzed by flow cytometry for expression of GFP.

Flow cytometric analysis

Analysis was performed on a Fortessa flow cytometer (BD Pharmingen, San Diego, CA). All antibodies were from Biolegend, except anti-Ki67 that was obtained from BD Pharmingen, anti-pErk 1/2 from Cell Signaling, and anti-rabbit 647 polyclonal from Life Technologies. Foxp3 and Ki67 staining was done with Foxp3 buffer staining kit obtained from eBioscience. Flow analysis was performed using FloJo software. For peripheral organs, analysis was done by gating on the lymphocyte gate based on FSC and SSC, followed by gating on $Ametrine^{+}TCR^{+}CD4^{+}$ cells; for thymic analysis, analysis was done after initially gating on lymphocytes, followed by gating on $Ametrine^{+}$ cells, and then on $CD4^{+}CD8^{-}$ T cells.

Statistical analysis

T cell receptor groups were ranked based on the 2D affinity and pErk point estimates. Each measure was given equal weight in a combined ranking calculated based on the sum of the individual rankings. Diabetes incidence curves were compared using log-rank test. All other group comparisons were done using the Kruskal-Wallis nonparametric test. Dunns post-test analysis was performed on all pairs for 2D affinity, or on selected pairs, comparing $InsB_{9\text{-}23}$-specific TCRs to the control 14H4 TCR, or higher affinity TCRs (P2, 1-10, 4-8, 3-4) to lower affinity TCRs (12-4.4, 12-4.4m1, 8-1.1), as noted in the figure legends. All correlation analyses, except Spearman correlation in Supplemental Table II, were based on Pearson correlation coefficients. For Spearman correlation analysis, mean values of each variable were taken for each T cell receptor. Spearman Correlation Coefficient was chosen because several of the variables included failed the Shapiro-Wilk test for normality. A significant p-value indicates that the correlation coefficient is statistically significantly different from zero. All statistical tests were two tailed, and p-values <0.05 were considered statistically significant (***$p \leq 0.001$, **$p \leq 0.01$, *$p \leq 0.05$). Statistical analyses were performed using Prism and SAS Version 9.2 (Cary, NC).

Results

Insulin-reactive TCRs possess a broad range of biophysical and functional affinities

TCR affinity can be assessed by determining the biophysical parameters of ligand:receptor interaction, as well as the relative functional biological outcomes of TCR ligation. We assembled a panel of eight $InsB_{9\text{-}23}$-specific TCRs, which were predominantly isolated from islet-resident T cells thereby ensuring physiological relevance (Supplemental Table I). Furthermore, all the TCRs selected can mediate T cell expansion or IL-2 secretion in response to the wild type $lnsB_{9\text{-}23}$ peptide. We used two expression systems to assess their biophysical, functional and diabetogenic potential. First, a TCR negative hybridoma was transduced with retrovirus encoding each of the insulin-specific TCRs or an irrelevant control (14H4 $HEL_{11\text{-}25}$ restricted TCR) plus a fluorescent protein (Supplemental Table I). Transductants were sorted to ensure comparable TCR cell surface expression. Second, we generated TCR retrogenic mice by transducing NOD.*scid* bone marrow with TCR-encoding

retrovirus that was subsequently used to reconstitute irradiated NOD.*scid* mice (20, 21, 23, 25).

The dominant diabetogenic $CD4^+$ insulin epitope $InsB_{9\text{-}23}$, like many other $CD4^+$ T cell epitopes, can bind into the MHC groove in several different registers (26-28). We assessed four recombinant MHC:peptide monomers, that had been modified using different approaches to stabilize their peptide register, for their capacity to stimulate T cell transductants. Since the wild type (WT) $InsB_{9\text{-}23}$ binds in a register that is recognized by most insulin-specific TCRs with fairly low affinity, the presumptive MHC anchor residues were modified to increase the peptide:MHC complex stability of this register (17, 28). The $InsB_{9}$_23(8G):H-$2A^{g7}$ monomer was selected for subsequent analysis based on the comparable responses observed with $InsB_{9\text{-}23}$- pulsed APC-stimulated TCR transductants (Supplemental Fig. 1C).

We first determined the biophysical and functional affinities of the $InsB_{9\text{-}23}$-specific TCRs. Biophysical measurements were obtained using the 2D micropipette adhesion frequency assay, a mechanical approach to measure TCR affinity between the T cell and a red blood cell coated with the stabilized $InsB_{9\text{-}23(8G)}$:H-$2A^{g7}$ monomer (10, 13, 17). The utilization of this approach in this study has allowed us to assess the affinity of multiple TCRs specific to the same antigenic peptide epitope. Importantly, the eight TCRs exhibited a range of statistically separable biophysical affinities that fell within the polyclonal range of TCR 2D affinities determined previously (Fig. 1A) (10, 15; unpublished data). The affinities calculated for insulin specific TCRs were relatively high compared to other self-reactive TCRs specific to myelin antigens (10^{-3}–10^{-4} compared to ~10^{-6} μm^4); however, they were similar to 2D affinities of other islet antigen specific TCRs (10, 14, 15); unpublished data). Still, it is unknown whether the eight TCRs span the entire range of affinities for $InsB_{9\text{-}23}$ represented by islet infiltrating T cells.

We next obtained functional affinities with TCR hybridoma transductants based on pErk activation and IL-2 secretion in response to $InsB_{9\text{-}23}$ peptide (Fig. 1B and Supplemental Fig. 1A). Importantly, there was a strong correlation between the functional affinity and the biophysical 2D affinity determined for all $InsB_{9\text{-}23}$-specific TCRs, except for 8-1.1 that appeared to mediate a surprisingly high pErk activation and IL-2 induction relative to its 2D affinity (Fig. 1C and Supplemental Fig. 1A). Although, the 2D affinities were on the upper end of what has been published for $CD4^+$ T cells in the 2D micropipette system, insulin-specific TCR transfectants responded only to high concentrations of WT peptide compared to the control non-self reactive TCR (Supplemental Fig. 1B). In order to facilitate subsequent comparison with other parameters, we arranged and color-coded the TCRs based on the ranking that incorporated the biophysical 2D affinity and functional affinity (Fig. 1D). Taken together, these data show a panel of $InsB_{9\text{-}23}$-specific TCRs that exhibit a broad range of physiologically relevant, correlative functional and biophysical affinities.

Diabetogenic potential exhibited over a broad range of TCR affinities

We next generated TCR retrogenic NOD.*scid* mice to determine the insulitic and diabetogenic potential of our panel of $InsB_{9\text{-}23}$-specific TCRs. We had previously shown that TCR specificity dictated T cell-autonomous islet infiltration (21). Consistent with these

findings, we observed that all the $InsB_{9-23}$-specific TCRs, but not the HEL_{11-25}-specific control TCR, were able to mediate T cell islet infiltration (Fig. 2A). Histological assessment of the pancreatic tissue sections confirmed extensive insulitis driven by almost all the TCRs, albeit with differing severity (Fig. 2B and 2C). Interestingly, the two TCRs mediating limited insulitis possessed the highest and one of the lowest TCR affinities (P2 and 12-4.4m1).

We next assessed the ability of the $InsB_{9-23}$-specific TCRs to induce spontaneous disease development in NOD.*scid* mice. We found that the majority of the TCRs (6 of 8) were able to induce spontaneous diabetes within 20 weeks post-retrogenic bone marrow transfer (Fig. 2D and 2E). Since most TCRs were isolated from infiltrated islets, the data suggest that a heterogenous population of T cells exhibiting a range of TCR affinities is involved in autoimmune organ destruction. Not surprisingly, P2 and 12-4.4m1, the two TCRs that mediated limited islet infiltration and insulitis, did not induce diabetes development, although, both P2 and 12-4.4m1 have the capacity to induce diabetes upon in vitro expansion, activation and transfer (Supplemental Fig. 2A). The remaining TCRs induced a surprisingly broad range of diabetes onset and incidence, with neither one of these parameters having any obvious correlation with TCR affinity or, by extension, the functional correlative above (Supplemental Fig. 2B and 2C). In essence all TCR affinities (whether high or low) isolated from islets have the potential to induce diabetes, but some intrinsic and/or extrinsic forces are influencing the outcome. There also appeared to be a trend, if not a direct correlation, between TCR affinity and the time of diabetes onset. For instance, the three that induced late onset had amongst the lowest TCR affinity (Fig. 2E and Supplemental Fig. 2C). Importantly, disease incidence did not correlate with the efficiency of bone marrow reconstitution, as determined by the percentage of $CD4^+$ T cells in PBMC with the same TCR or in general for all the TCRs examined (Supplemental Fig. 2 D). Most of the T cells infiltrating the pancreatic islets exhibited Th1 type cytokine expression with high expression of IFNγ upon restimulation *in vitro* and minimal expression of IL-17 and IL-4, and IL-10 (Supplemental Fig. 2E and data not shown). Taken together, these data suggest that autoimmune diabetes can be mediated by TCRs with a relatively broad affinity range, and that TCR affinity alone may be a poor predictor of $CD4^+$ T cell diabetogenic potential.

TCR affinity defines signal strength and shapes T cell development in vivo

We next assessed the impact of TCR affinity on the development of $InsB_{9-23}$-specific T cells. Although all eight insulin TCRs were able to support $CD4^+$ T cell development, efficiency was highly variable (Fig. 3A). Interestingly, higher TCR affinities were trending with lower TCR expression raising the possibility that increased negative selection pressure for the higher affinity TCRs may select for thymic emigration of T cells with lower TCR levels (Fig. 3 B). These data suggest that autoreactive T cells exhibiting a range of TCR affinities are able to largely escape negative selection.

Previous studies have shown that expression of the inhibitory signaling receptor CD5 on double positive (DP) and SP thymocytes is controlled by TCR avidity, directly correlates with TCR signal strength, and thus reactivity to self (29-31). The level of CD5 expression on

the surface of T cells was variable among the TCRs, but largely consistent among the organs of the same TCR (Fig. 3C). For the most part, 2D TCR affinity correlated with the level of CD5 expression, with two notable exceptions, 8-1.1 and 12-4.4m1 (Fig. 3C). The response of 8-1.1 T cells to WT $InsB_{9\text{-}23}$ peptide was more closely aligned with CD5 expression than 2D TCR affinity (Fig. 3E and 3F). Overall, CD5 expression correlated better with the response to WT exogenous peptide than to 2D TCR affinity (Fig. 3E and 3F). These data suggest that $CD4^+$ T cell responses to $InsB_{9\text{-}23}$ in the thymus are driven by TCR affinity, and the TCR signaling threshold may be partially normalized among the $InsB_{9\text{-}23}$-specific TCRs by adjusting levels of CD5 expression (32). In combination, TCR 2D affinity, *in vitro* response to antigenic peptide, and *in vivo* CD5 expression segregate the eight $InsB_{9\text{-}23}$-specific TCRs into two distinct groups based on their relative sensitivity to antigen. P2, 1-10, 4-8, and 3-4 showed higher overall affinity to antigen; 12-4.4, 8-1.1, 12-4.1 and 12-4.4m1 exhibited overall lower affinity.

In order to assess the impact of TCR affinity on TCR signaling *in vivo*, we expressed $InsB_{9\text{-}23}$-specfic TCRs on a NOD.*scid*.$Nur77^{GFP}$ background to facilitate quantification of pErk activation via the early immediate downstream gene Nur77 (33). There was a correlative trend between TCR affinity and GFP expression in thymocytes (Fig. 3D). The overall level of GFP expression in the thymus was also similar to the peripheral non-draining lymph nodes and spleen. Interestingly, the level of GFP expression was substantially increased in the draining pancreatic lymph nodes (PLN), consistent with increased antigen availability. However, there was minimal correlation between GFP expression in the PLN and 2D TCR affinity (Fig. 3G). Interestingly, upon T cell islet infiltration GFP expression was comparable amongst all $InsB_{9\text{-}23}$-specific TCRs, suggesting that in an inflammatory setting environmental signals compensate for varying TCR affinity. There was no correlation between CD5 and $Nur77^{GFP}$ expression in the draining LN (data not shown).

Since we have amassed a large dataset comparing the *in vivo* function of eight $InsB_{9\text{-}23}$-specific TCRs, we performed a simultaneous correlative analysis of multiple parameters associated with TCR affinity obtained from our study (Supplementary Table II). The spearman rank correlation coefficients were used to rank the strength of correlation of the TCR functional parameters, including TCR affinity and disease development. Effective 2D TCR affinity correlated strongly with the strength of TCR signaling in the thymus, as assessed by the level of $Nur77^{GFP}$ expression (*r = 0.7381), and downregulation of TCR expression (negative correlation with the level of TCR expression in the thymus (*r = −0.738), and spleen (*r = −0.929)). The strongest correlation was observed between CD5 expression in the islets and PLN (*r = 1). CD5 expression in the thymus was also correlated with both islets and PLN (*r = 0.6667), which suggests that CD5 levels are stabilized in the periphery and do not change after prolonged stimulation in the islets. Interestingly, CD5 expression correlated with the frequencies of $CD4^+$ T cells in the spleen and PBMCs (*r = 0.7619, *r = 0.8095), which suggests that T cell accumulation in the peripheral organs is positively associated with the strength of TCR signaling. However, diabetes incidence did not show a strong correlation with any parameter associated with TCR affinity, and only

correlated with the level of insulitis, and the frequency and number of infiltrating $CD4^+$ T cells (*r = 0.8264; *r = 0.8024; *r = 0.7306 respectively).

Tolerance mechanisms preferentially affect higher affinity diabetogenic TCRs

Even though TCR affinity for the most part correlated with *in vivo* and *in vitro* TCR signaling in response to antigen (Fig. 1C and 3F), we observed only minimal correlation between TCR affinity and disease incidence or onset: specifically, lack of any diabetes onset for the highest and one of the lowest affinity TCRs (P2 and 12-4.4m1), and delayed onset for the lower affinity TCRs (8-1.1 and 12-4.1) (Supplemental Fig. 2B and 2C). We postulated that downstream signaling after initial TCR stimulation might lead to activation of negative regulatory feedback mechanisms, including variable expression of CD5, which normalizes the level of TCR signaling during chronic disease progression among high and low affinity TCRs. This would be consistent with normalization of $Nur77^{GFP}$ expression in T cells that have been recruited to the pancreatic islets (Fig. 3D). We therefore assessed the *in vitro* response of T cells lines derived from $Nur77^{GFP}$ mice to WT peptide and also to naturally processed insulin under controlled stimulation conditions. $Nur77^{GFP}$ expression after 24 hours in culture with antigens and APCs was analyzed by flow cytometry (Fig. 4A). There was a significant correlation between pErk activation in transfectants and GFP expression in the T cell lines in response to WT peptide (Fig. 4B and 4C), although the discordance between these values suggested modification of TCR signaling in T cells. Interestingly, T cell response to whole protein best correlated with *in vivo* GFP expression in the draining lymph nodes over CD5 or 2D affinity (Fig. 4B and 4D), which supported our hypothesis that there is activation of feedback negative regulatory mechanisms that modulate TCR signaling *in vivo* and *in vitro.* Moreover, the spearman correlation analysis showed that 2D affinity correlated with response to protein stimulation when it was normalized to anti-CD3 stimulation (Supplementary Table II, $Nur77^{GFP}$, insulin; *r = 0.7857), which suggests that $InsB_{9\text{-}23(8G)}$:H2-A^{g7} monomer used for measurements of 2D affinity closely mimics the naturally processed epitope, and supports our hypothesis that there are permanent regulatory changes downstream of TCR ligation modulating signaling in the higher affinity TCRs (Supplementary Table II). We therefore assessed the role of canonical central and peripheral tolerance mechanisms in regulating diabetogenic potential.

First, NOD.*Ins2*$^{-/-}$ mice develop accelerated and exacerbated autoimmune diabetes (34, 35). Deletion of the *Ins2* gene, which is expressed in both the thymus and pancreas, unlike the *Ins1* gene, which is only expressed in the pancreas, results in increased susceptibility to diabetes largely due to inefficient deletion of insulin-reactive clones during thymic selection (35). We expressed the panel of $InsB_{9\text{-}23}$-specific TCRs in NOD.*scid.Ins2*$^{-/-}$ mice. Strikingly, there was a clear impact of Ins2-mediated central tolerance on T cells expressing predominantly high but not low affinity TCRs (Fig. 5). Interestingly, the highest affinity TCR P2 did not show any disease development on the NOD.*scid.Ins2*$^{-/-}$ background. However, upon *in vitro* activation and expansion and subsequent adoptive transfer P2 T cells are capable of inducing diabetes to some extent (Supplemental Fig. 2A), suggesting that additional parameters other than Ins2-mediated central tolerance in the thymus regulate its pathogenic potential. Although the impact of *Ins2*$^{-/-}$ background on diabetogenic potential of high affinity TCR was dramatic, we did not notice any obvious changes in thymic

selection based on frequency or number of SP CD4+ thymocytes, TCR or CD5 expression (data not shown).

Second, we examined the contribution of Foxp3$^+$ regulatory T (Treg) cell-mediated peripheral tolerance to disease outcome in InsB$_{9\text{-}23}$-specific TCR retrogenic mice. Treg cell accumulation was observed in the periphery of all InsB$_{9\text{-}23}$-specific TCR retrogenic mice, albeit over a broad range (0.5-12%), while a more consistent Treg cell percentage was observed in the PLN (1.5-5%; Fig. 6A). Interestingly, there appeared to be a trend towards higher Treg cell percentages, especially in the islets, of mice expressing high affinity TCRs. Based on the spearman correlation analysis, frequencies of Foxp3$^+$ T cells in the islets were associated with CD5 expression in the thymus and CD4$^+$ T cells frequency and number in the periphery (Supplementary Table II; *r = 0.7143, *r = 0.7381, *r = 0.7143), which points to the positive association of TCR strength of signal and/or T cell numbers and Treg accumulation in the inflammatory setting. While the proportion of Treg cells that are thymically or peripherally derived was not determined, there appeared to be no alteration of Helios expression on Tregs with different TCR affinities.

We then assessed the contribution of these Treg cell populations in moderating autoimmune diabetes by their selective deletion in NOD.*scid*.Foxp3^{DTR} TCR retrogenic mice following diphtheria toxin treatment from 5.5 weeks post bone marrow transfer (18). Synonymous with the observations made in the NOD.*scid.Ins2*$^{-/-}$ experiments above, a selective contribution of Foxp3$^+$ Treg cells was observed in mice expressing higher affinity InsB$_{9\text{-}23}$-specific TCRs (1-10, 3-4 and 4-8; Fig. 6B). It is not clear whether the impact of Tregs in high affinity TCR retrogenic mice was due to the increased number of Tregs or the increased suppressive capacity of those Tregs due to their higher affinity TCR. The rate of disease acceleration was different among the three TCRs, and slower than was observed for the BDC2.5/NOD.Foxp3^{DTR} mice, which was probably due to the differences in Treg / T effector ratio or function of cells with variable TCR affinities, different antigenic specificities (for BDC2.5), and/or wider Treg TCR repertoire (18). Taken together, these data suggest that central and peripheral tolerance mechanisms selectively impinge on the pathogenicity of autoreactive TCRs with higher affinity to mitigate their diabetogenic potential to a level comparable to TCRs with lower affinity.

Discussion

In this study, we assessed whether the biophysical properties of the TCR, such as affinity, alone can determine the autoimmune pathogenicity of T cells or whether other factors converge to shape disease outcome. Previous efforts to address this important but often contentious issue have been limited by the number of TCRs examined (6-10). We have overcome this barrier by using TCR retrogenic technology to generate mice expressing one of eight InsB$_{9\text{-}23}$-specific TCRs with a broad affinity range. This approach has three key advantages: (1) any genetic background can be used, which remains consistent between groups, (2) multiple TCRs can be simultaneously analyzed, and (3) a panel of TCRs to a single T cell epitope can be analyzed. Surprisingly our study showed that 2D TCR affinity did not predict disease outcome. In fact both high and low affinity TCRs, at least within the range assessed, caused significant insulitis and autoimmune diabetes. These data also

suggest that relatively small changes in 2D TCR affinity (within 10-fold range) can result in a very broad range of biological, regulatory and pathogenic outcomes. Given that most of the TCRs used in this study were directly derived from islet infiltrating T cells, an autoimmune $CD4^+$ T cell population specific for a single self-epitope can be composed of highly pathogenic, non-pathogenic and regulatory clonal populations.

The 2D functional affinities we obtained for islet-infiltrating $InsB_{9\text{-}23}$-specific TCRs are relatively high compared to other published autoreactive TCR 2D affinities (10^{-3}–10^{-4} vs. 10^{-5} μm^4), and are similar to non-autoimmune antigen-specific TCRs (10, 13-15). These TCRs may preferentially recognize insulin peptide bound in the non-favorable register 3 (27), and *in vivo* the instability of this complex probably has some effect on the dwell time of the TCR, thus allowing escape of $InsB_{9\text{-}23}$-specific T cells from negative selection in the thymus. Indeed, many of these TCRs only respond to relatively high levels of antigen *in vitro*. Similarly, human $InsA_{1\text{-}15}$-specific T cells cloned from pancreatic islets of type 1 diabetic patients were activated only with high levels of antigenic peptide (36). Thus, it is possible that $InsB_{9\text{-}23}$-specific $CD4^+$ T cell pathogenicity is governed more by the efficiency with which this epitope can be loaded into H-$2A^{g7}$ in the 3rd register and presented to T cells that TCR affinity *per se*. It is also possible that peptide loading may be more efficiently in the islets and/or PLN compared thymus due to the differing microenvironments (37). Given that all of the TCRs were isolated based on T cell reactivity to insulin, it is possible that we missed lower affinity TCRs that are present during islet infiltration and may contribute to the disease. Future studies with polyclonal populations analyzed using sensitive 2D TCR affinity measurements will be required to fully address this issue.

Central and peripheral tolerance mechanisms collaborate to limit autoimmune insults. However, the extent to which they shape the clonal diversity of an autoimmune response is poorly understood. Our results and a previous study (38) are somewhat different to the data obtained with model antigens where negative selection has a sharp and well-defined affinity threshold (5). Higher affinity $InsB_{9\text{-}23}$-specific TCRs (especially P2) are affected by the level of antigen expressed in the thymus such that they are rendered non pathogenic unless activated *in vitro*, but complete deletion is not observed. Thus, thymically expressed insulin has a partial effect on negative selection in contrast to the well-studied thymic selection events mediated by the male HY antigen. Likewise, a surprising large proportion of $InsB_{9\text{-}23}$-specific TCRs can navigate negative selection and induce autoimmune diabetes over a seemingly broad TCR affinity range. However, it was evident from our study that intra-thymically expressed insulin appeared to preferentially impact the pathogenicity of higher affinity $InsB_{9\text{-}23}$-specific TCR while having no obvious effect on low affinity TCRs. Thus, autoantigen expression in the thymus may inadvertently contribute to shaping and broadening the polyclonal autoimmune response.

Previous studies have shown that peripheral negative regulators can affect TCR pathogenicity in autoimmune models (6, 39). Our study suggests that minor differences in TCR affinity in $InsB_{9\text{-}23}$-specific $CD4^+$ T cells influence their pathogenicity and the extent to which they are affected by negative regulatory mechanisms, such as Treg cells. Interestingly, high affinity TCRs are more susceptible to Treg cell-mediated peripheral tolerance mechanisms. With one exception (12-4.4m1), higher affinity TCRs displayed

increased frequencies of Foxp3$^+$ T cells accumulating in the pancreatic islets, which is consistent with the idea that Treg development is associated with high affinity TCRs (40). This suggests that the Treg cell/T effector cell ratio in the islets defines the extent of autoimmune diabetes and may provide the simplest explanation for the impact of Treg cell deletion on pathogenicity. It is possible that the reduced susceptibility of T cells to Treg cell-mediated regulation in the later stages of chronic autoimmune disease is due in part to accumulation of lower affinity T cells that are less likely to be converted into a regulatory populations and are more refractory to regulation due to their reduced intrinsic inhibitory mechanisms.

In conclusion, our study shows that the diabetogenic potential of CD4$^+$ T cells is not exclusively governed by TCR affinity and that T cell clones with both high and low affinity TCR can mediate potent pathogenic responses. The mechanistic basis for this lies in the differential effect of central and peripheral tolerance mechanisms that preferential impinge on the diabetogenic potential of high affinity TCRs, thereby ‘leveling the playing field’. This may inadvertently broaden the autoreactive T cell repertoire to a single epitope where higher and lower affinity T cells may exhibit similar pathogenicity. Whether these criteria shape the human autoimmune response in type 1 diabetes, or any other autoimmune disease, remains to be determined. However, if the observations made here represent a general principle, it is conceivable that multiple combinatorial approaches may have to be used to induce effective, broad, long-term tolerance in the clinic.

Supplementary Material

Refer to Web version on PubMed Central for supplementary material.

Acknowledgments

The authors would like to thank members of the Vignali lab for assistance with harvesting bone marrow and helpful discussions; Richard Cross, Stephanie Morgan, Greig Lennon and Parker Ingle for cell sorting; Scott Brown for assistance with generating T cell fusions; John Altman and Richard Willis, National Institutes of Health Tetramer Core Facility, for providing peptide and major histocompatibility complex monomers; the staff of the Shared Animal Resource Center at St. Jude for the animal husbandry; and the Hartwell Center for Biotechnology and Bioinformatics at St. Jude for primers and sequencing.

This work was supported by the National Institutes of Health (DK089125 to D.A.A.V.), Juvenile Diabetes Research Foundation (3-2009-594 and 10-2013-73 to M.B.), NCI Comprehensive Cancer Center Support CORE grant (CA21765, to D.A.A.V.), and ALSAC (to D.A.A.V.). Abbreviations used in this article: 2D, two-dimensional; GFP, green fluorescent protein; DN, double negative; SP, single positive; LN, lymph nodes; PLN, pancreatic lymph node; NOD, non-obese diabetic; Treg, T regulatory cell; SPF, special pathogen free.

References

1. Davis MM, Boniface JJ, Reich Z, Lyons D, Hampl J, Arden B, Chien Y. Ligand recognition by alpha beta T cell receptors. Annu Rev Immunol. 1998; 16:523–544. [PubMed: 9597140]
2. Williams CB, Engle DL, Kersh GJ, Michael White J, Allen PM. A kinetic threshold between negative and positive selection based on the longevity of the T cell receptor-ligand complex. J Exp Med. 1999; 189:1531–1544. [PubMed: 10330432]
3. Cole DK, Pumphrey NJ, Boulter JM, Sami M, Bell JI, Gostick E, Price DA, Gao GF, Sewell AK, Jakobsen BK. Human TCR-binding affinity is governed by MHC class restriction. J Immunol. 2007; 178:5727–5734. [PubMed: 17442956]

4. van der Merwe PA, Davis SJ. Molecular interactions mediating T cell antigen recognition. Annu Rev Immunol. 2003; 21:659–684. [PubMed: 12615890]
5. Palmer E, Naeher D. Nat Rev Immunol. 2009; Affinity threshold for thymic selection through a T-cell receptor-co-receptor zipper.9:207–213. [PubMed: 19151748]
6. Gronski MA, Boulter JM, Moskophidis D, Nguyen LT, Holmberg K, Elford AR, Deenick EK, Kim HO, Penninger JM, Odermatt B, Gallimore A, Gascoigne NR, Ohashi PS. TCR affinity and negative regulation limit autoimmunity. Nat Med. 2004; 10:1234–1239. [PubMed: 15467726]
7. Amrani A, Verdaguer J, Serra P, Tafuro S, Tan R, Santamaria P. Progression of autoimmune diabetes driven by avidity maturation of a T-cell population. Nature. 2000; 406:739–742. [PubMed: 10963600]
8. Standifer NE, Burwell EA, Gersuk VH, Greenbaum CJ, Nepom GT. Changes in autoreactive T cell avidity during type 1 diabetes development. Clin Immunol. 2009; 132:312–320. [PubMed: 19482555]
9. Malherbe L, Hausl C, Teyton L, McHeyzer-Williams MG. Clonal selection of helper T cells is determined by an affinity threshold with no further skewing of TCR binding properties. Immunity. 2004; 21:669–679. [PubMed: 15539153]
10. Sabatino JJ Jr. Huang J, Zhu C, Evavold BD. High prevalence of low affinity peptide-MHC II tetramer-negative effectors during polyclonal CD4+ T cell responses. J Exp Med. 2011; 208:81–90. [PubMed: 21220453]
11. Blanchfield JL, Shorter SK, Evavold BD. Monitoring the Dynamics of T Cell Clonal Diversity Using Recombinant Peptide:MHC Technology. Front Immunol. 2013; 4:170. [PubMed: 23840195]
12. Adams JJ, Narayanan S, Liu B, Birnbaum ME, Kruse AC, Bowerman NA, Chen W, Levin AM, Connolly JM, Zhu C, Kranz DM, Garcia KC. T cell receptor signaling is limited by docking geometry to peptide-major histocompatibility complex. Immunity. 2011; 35:681–693. [PubMed: 22101157]
13. Huang J, Zarnitsyna VI, Liu B, Edwards LJ, Jiang N, Evavold BD, Zhu C. The kinetics of two-dimensional TCR and pMHC interactions determine T-cell responsiveness. Nature. 2010; 464:932–936. [PubMed: 20357766]
14. Rosenthal KM, Edwards LJ, Sabatino JJ Jr. Hood JD, Wasserman HA, Zhu C, Evavold BD. Low 2-dimensional CD4 T cell receptor affinity for myelin sets in motion delayed response kinetics. PLoS One. 2012; 7:e32562. [PubMed: 22412888]
15. Schubert DA, Gordo S, Sabatino JJ Jr. Vardhana S, Gagnon E, Sethi DK, Seth NP, Choudhuri K, Reijonen H, Nepom GT, Evavold BD, Dustin ML, Wucherpfennig KW. Self-reactive human CD4 T cell clones form unusual immunological synapses. J Exp Med. 2012; 209:335–352. [PubMed: 22312112]
16. Huang J, Edwards LJ, Evavold BD, Zhu C. Kinetics of MHC-CD8 interaction at the T cell membrane. J Immunol. 2007; 179:7653–7662. [PubMed: 18025211]
17. Crawford F, Stadinski B, Jin N, Michels A, Nakayama M, Pratt P, Marrack P, Eisenbarth G, Kappler JW. Specificity and detection of insulin-reactive CD4+ T cells in type 1 diabetes in the nonobese diabetic (NOD) mouse. Proc Natl Acad Sci U S A. 2011; 108:16729–16734. [PubMed: 21949373]
18. Feuerer M, Shen Y, Littman DR, Benoist C, Mathis D. How punctual ablation of regulatory T cells unleashes an autoimmune lesion within the pancreatic islets. Immunity. 2009; 31:654–664. [PubMed: 19818653]
19. Arnold PY, Burton AR, Vignali DA. J Immunol. 2004; Diabetes incidence is unaltered in glutamate decarboxylase 65-specific TCR retrogenic nonobese diabetic mice: generation by retroviral-mediated stem cell gene transfer.173:3103–3111. [PubMed: 15322170]
20. Burton AR, Vincent E, Arnold PY, Lennon GP, Smeltzer M, Li CS, Haskins K, Hutton J, Tisch RM, Sercarz EE, Santamaria P, Workman CJ, Vignali DA. On the pathogenicity of autoantigen-specific T-cell receptors. Diabetes. 2008; 57:1321–1330. [PubMed: 18299317]
21. Lennon GP, Bettini M, Burton AR, Vincent E, Arnold PY, Santamaria P, Vignali DA. T cell islet accumulation in type 1 diabetes is a tightly regulated, cell-autonomous event. Immunity. 2009; 31:643–653. [PubMed: 19818656]

22. Bettini M, Castellaw AH, Lennon GP, Burton AR, Vignali DA. Prevention of autoimmune diabetes by ectopic pancreatic beta-cell expression of interleukin-35. Diabetes. 2012; 61:1519–1526. [PubMed: 22427377]
23. Bettini ML, Bettini M, Nakayama M, Guy CS, Vignali DA. Generation of T cell receptor-retrogenic mice: improved retroviral-mediated stem cell gene transfer. Nat Protoc. 2013; 8:1837–1840. [PubMed: 24008379]
24. Leiter EH. Coligan, John E.The NOD mouse: a model for insulin-dependent diabetes mellitus. Current protocols in immunology. 2001 [et al.] Chapter 15: Unit 15 19.
25. Holst J, Vignali KM, Burton AR, Vignali DA. Rapid analysis of T-cell selection in vivo using T cell-receptor retrogenic mice. Nat Methods. 2006; 3:191–197. [PubMed: 16489336]
26. Bankovich AJ, Girvin AT, Moesta AK, Garcia KC. Mol Immunol. 2004; Peptide register shifting within the MHC groove: theory becomes reality.40:1033–1039. [PubMed: 15036907]
27. Stadinski BD, Zhang L, Crawford F, Marrack P, Eisenbarth GS, Kappler JW. Diabetogenic T cells recognize insulin bound to IAg7 in an unexpected, weakly binding register. Proc Natl Acad Sci U S A. 2010; 107:10978–10983. [PubMed: 20534455]
28. Mohan JF, Petzold SJ, Unanue ER. Register shifting of an insulin peptide-MHC complex allows diabetogenic T cells to escape thymic deletion. J Exp Med. 2011; 208:2375–2383. [PubMed: 22065673]
29. Azzam HS, Grinberg A, Lui K, Shen H, Shores EW, Love PE. CD5 expression is developmentally regulated by T cell receptor (TCR) signals and TCR avidity. J Exp Med. 1998; 188:2301–2311. [PubMed: 9858516]
30. Smith K, Seddon B, Purbhoo MA, Zamoyska R, Fisher AG, Merkenschlager M. Sensory adaptation in naive peripheral CD4 T cells. J Exp Med. 2001; 194:1253–1261. [PubMed: 11696591]
31. Mandl JN, Monteiro JP, Vrisekoop N, Germain RN. T cell-positive selection uses self-ligand binding strength to optimize repertoire recognition of foreign antigens. Immunity. 2013; 38:263–274. [PubMed: 23290521]
32. Perez-Villar JJ, Whitney GS, Bowen MA, Hewgill DH, Aruffo AA, Kanner SB. CD5 negatively regulates the T-cell antigen receptor signal transduction pathway: involvement of SH2-containing phosphotyrosine phosphatase SHP-1. Mol Cell Biol. 1999; 19:2903–2912. [PubMed: 10082557]
33. Moran AE, Holzapfel KL, Xing Y, Cunningham NR, Maltzman JS, Punt J, Hogquist KA. T cell receptor signal strength in Treg and iNKT cell development demonstrated by a novel fluorescent reporter mouse. J Exp Med. 2011; 208:1279–1289. [PubMed: 21606508]
34. Thebault-Baumont K, Dubois-Laforgue D, Krief P, Briand JP, Halbout P, Vallon-Geoffroy K, Morin J, Laloux V, Lehuen A, Carel JC, Jami J, Muller S, Boitard C. Acceleration of type 1 diabetes mellitus in proinsulin 2-deficient NOD mice. J Clin Invest. 2003; 111:851–857. [PubMed: 12639991]
35. Moriyama H, Abiru N, Paronen J, Sikora K, Liu E, Miao D, Devendra D, Beilke J, Gianani R, Gill RG, Eisenbarth GS. Evidence for a primary islet autoantigen (preproinsulin 1) for insulitis and diabetes in the nonobese diabetic mouse. Proc Natl Acad Sci U S A. 2003; 100:10376–10381. [PubMed: 12925730]
36. Kent SC, Chen Y, Bregoli L, Clemmings SM, Kenyon NS, Ricordi C, Hering BJ, Hafler DA. Expanded T cells from pancreatic lymph nodes of type 1 diabetic subjects recognize an insulin epitope. Nature. 2005; 435:224–228. [PubMed: 15889096]
37. Mohan JF, Levisetti MG, Calderon B, Herzog JW, Petzold SJ, Unanue ER. Unique autoreactive T cells recognize insulin peptides generated within the islets of Langerhans in autoimmune diabetes. Nature immunology. 2010; 11:350–354. [PubMed: 20190756]
38. Fousteri G, Jasinski J, Dave A, Nakayama M, Pagni P, Lambolez F, Juntti T, Sarikonda G, Cheng Y, Croft M, Cheroutre H, Eisenbarth G, von Herrath M. Following the fate of one insulin-reactive CD4 T cell: conversion into Teffs and Tregs in the periphery controls diabetes in NOD mice. Diabetes. 2012; 61:1169–1179. [PubMed: 22403296]
39. Feuerer M, Hill JA, Mathis D, Benoist C. Foxp3+ regulatory T cells: differentiation, specification, subphenotypes. Nat Immunol. 2009; 10:689–695. [PubMed: 19536194]

40. Gottschalk RA, Corse E, Allison JP. TCR ligand density and affinity determine peripheral induction of Foxp3 in vivo. J Exp Med. 2010; 207:1701–1711. [PubMed: 20660617]

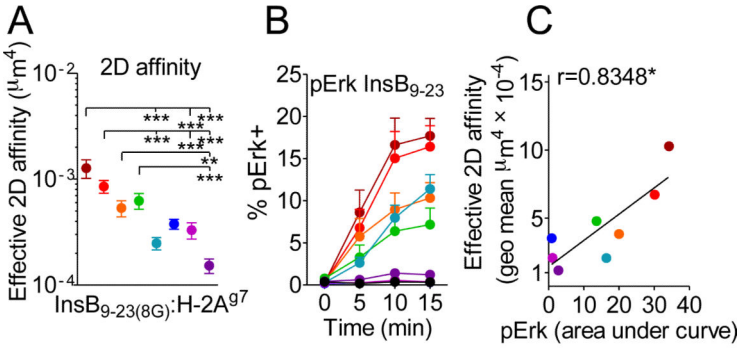

D

T cell receptor	2D affinity rank	pErk rank	sum of ranks	combined rank
P2	1	1	2	1
1-10	2	2	4	2
4-8	4	3	7	3
3-4	3	5	8	4
8-1.1	7	4	11	5
12-4.4	5	7	12	6
12-4. 4_{m1}	6	7	13	7
12-4.1	8	6	14	8

P2
1-10
4-8
3-4
8-1.1
12-4.4
12-4.4m1
12-4.1

FIGURE 1. Functional and biophysical affinity measurements for $InsB_{9-23}$-specific TCRs

(A) 2D TCR biophysical affinity was measured as described previously (Huang J. et. al. 2010) for retrogenic $CD4^+$ T cell lines. At least two unique cell lines were used to calculate 2D affinity on separate days; each dot represents geometric mean of affinities measured for at least 12 different T cells, error bars represent SEM.

(B) TCR^-CD4^+ 4G4 hybridoma was transfected with TCRs, sorted on comparable TCR expression level, and stimulated with $InsB_{9-23}$. pErk response was used as a readout of functional affinity. An average of at least four separate experiments generated with three separate cells lines is depicted. Error bars represent SEM.

(C) Correlation between TCR 2D affinity and pErk expression (calculated as an area under the line from panel B). (D) Ranking of the TCRs based on combination of pErk and 2D affinity.

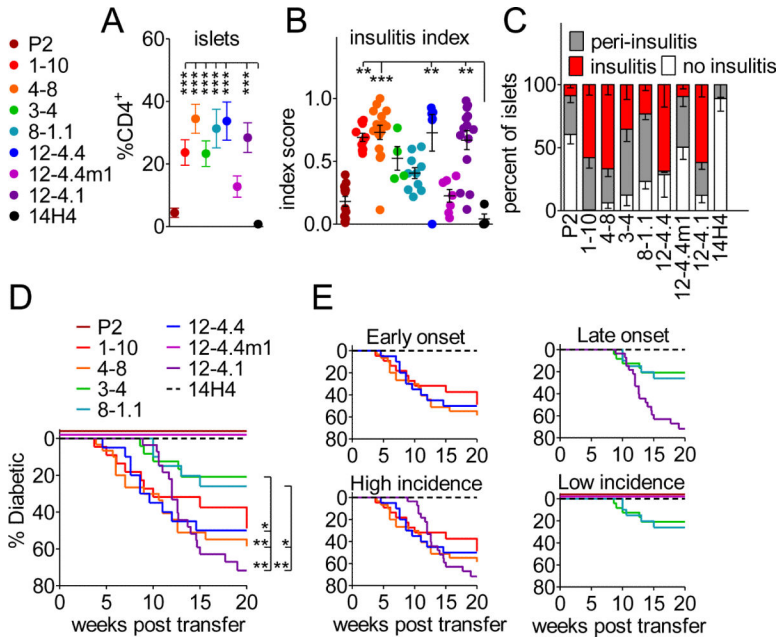

FIGURE 2. High and low affinity TCRs are able to accumulate in the pancreas and induce spontaneous diabetes development

(A) Frequencies of insulin specific T cells in the infiltrated pancreatic islets were obtained from analysis of TCR retrogenic mice 7-8 weeks post bone marrow transfer. An average of at least 10 mice from 4 separate experiments is shown. Error bars represent SEM.

(B and C) Histological assessment of insulitis in insulin TCR retrogenic mice at 8-9 weeks post bone marrow transfer.

(D) TCR retrogenic mice were monitored for spontaneous diabetes development ($n \geq 20$ mice per group).

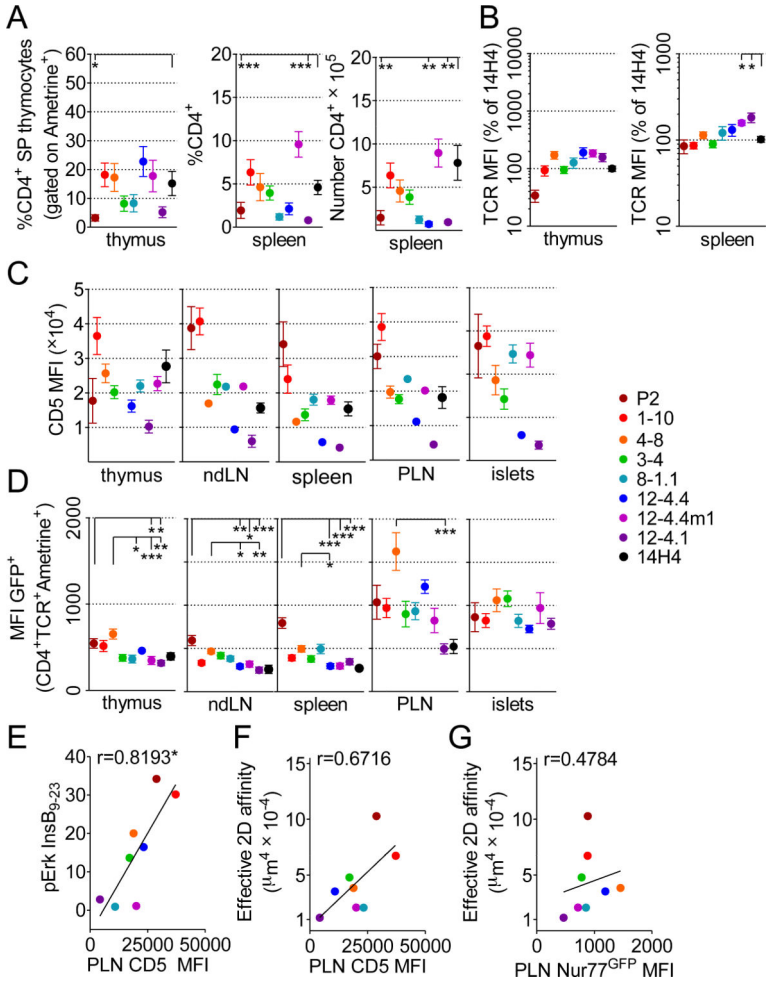

FIGURE 3. CD5 and Nur77^{GFP} expression on insulin specific CD4^{+} T cells in the thymus, peripheral lymphoid organs and infiltrated pancreatic islets

(A) Frequencies of CD4^{+} SP in thyme, and frequency and number of CD4^{+} T cells in the spleens of TCR retrogenic mice analyzed at 7-8 weeks post bone marrow transfer. An average of at least 9 mice and 4 separate experiments is shown. Error bars represent SEM.

(B) Relative TCR expression levels were calculated based on average TCR expression for 14H4 in the same experiment. At least 8 separate mice from 4 separate experiments were analyzed.

(C) CD5 expression by insulin specific T cells in the thymus, spleen and infiltrated pancreatic islets. An average of at least 7 mice from 3 separate experiments is shown. Error bars represent SEM.

(D) Nur77^{GFP} expression by insulin specific T cells in the thymus, peripheral lymphoid organs and infiltrated pancreatic islets. An average of at least 7 mice from 3 different experiments is shown. Error bars represent SEM.

(E) Correlation between transfectant pErk response to WT peptide calculated from Fig. 1B and average CD5 expression in the draining lymph nodes.

(F) Correlation between 2D affinity and average CD5 expression in the draining lymph nodes.

(G) Correlation between 2D TCR affinity and Nur77^{GFP}.

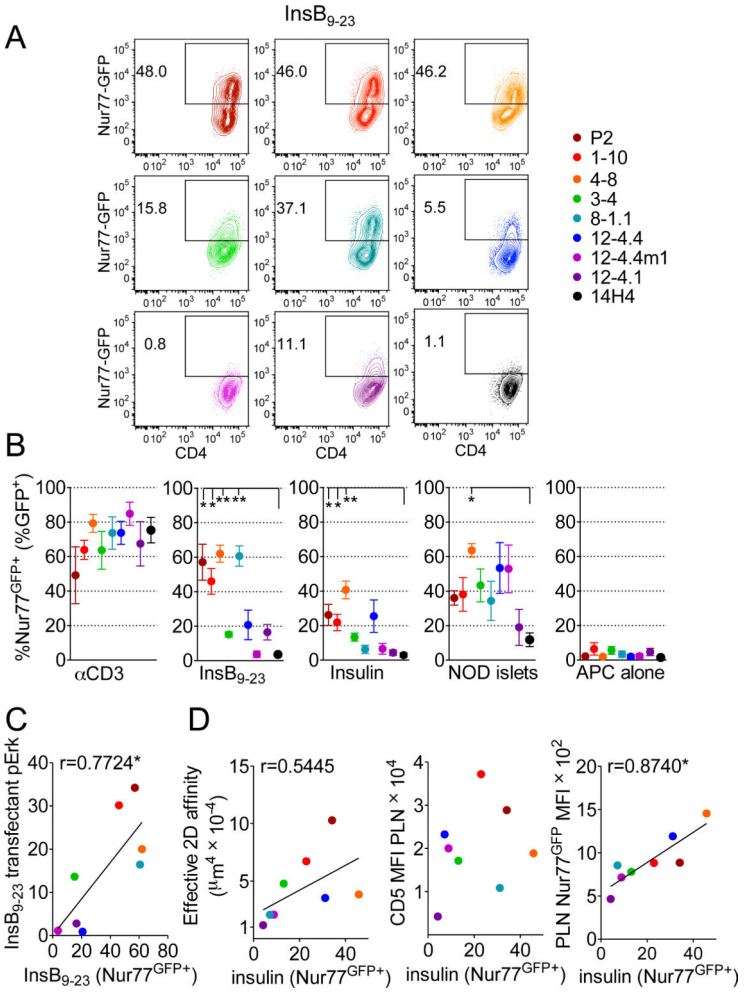

FIGURE 4. ***In vitro*** **readout of TCR stimulation via Nur77^{GFP} reporter**

Insulin specific T cell lines developed from Nur77^{GFP} TCR retrogenic mice were stimulated for 24 hrs in vitro with WT peptide, whole protein (insulin), or NOD islets in combination with exogenous splenocytes; after which cells were analyzed for Nur77^{GFP} expression as a readout of TCR activation.

(A) Representative flow plots for cell line stimulation with insulin. (B) GFP upregulation in response to stimuli. (C) Correlation between transfectant pErk activation and T cell Nur77^{GFP} expression in response to WT peptide. (D) Correlations between 2D affinity, CD5 expression in PLN, and Nur77^{GFP} expression compared to T cell response to naturally processed insulin.

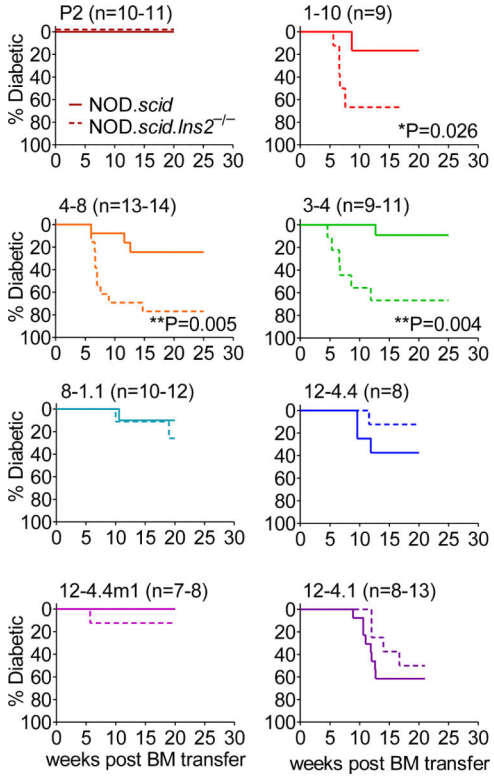

FIGURE 5. Accelerated diabetes development in TCR retrogenic mice on the Ins2−/− background is more dramatic for high affinity TCRs

TCR retrogenic NOD.*scid* bone marrow was transferred to NOD.*scid* or NOD.*scid.Ins2−/−* recipients. Frequency of peripheral $CD4^+Ametrine^+TCR^+$ T cells was used to verify equal reconstitution between groups. TCR retrogenic mice were monitored for diabetes development. At least 7 mice per group were monitored for spontaneous diabetes development.

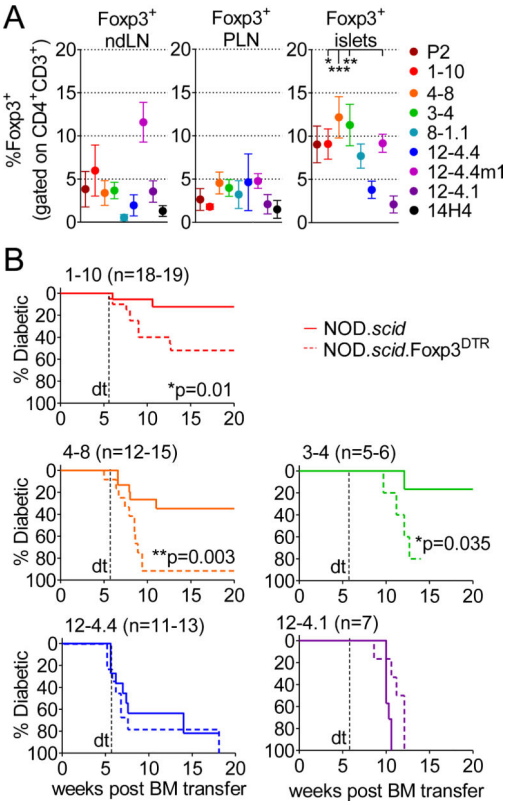

FIGURE 6. Deletion of Foxp3^{+} CD4^{+} T cells in insulin TCR retrogenic mice leads to accelerated diabetes development in higher affinity TCRs

(A) Foxp3^{+} T cells accumulate in the pancreatic islets of TCR retrogenic mice: frequency of Foxp3^{+} T cells was assessed in lymph nodes and pancreatic islets of TCR retrogenic mice 8 weeks post bone marrow transfer. Analysis shown is for at least 5 mice per group.

(B) TCR retrogenic mice were generated with NOD.*scid* or NOD.*scid*.Foxp3^{DTR+} bone marrow. Frequency of peripheral CD4^{+}Ametrine^{+}TCR^{+} T cells was used to verify equal reconstitution between groups. Mice were treated with diphtheria toxin twice a week starting at 5.5 weeks post bone marrow transfer and monitored for diabetes development.